

The Roll Decay of Floating Cylinders with Bilge Keels

R. K. M. Seah, T. Celano and R. W. Yeung

Mechanical Engineering & Ocean Engineering

University of California at Berkeley

Berkeley, California 94720-1740, USA

1 Introduction

While there are substantial interests in the motion of floating bodies in waves, the transient, free response of floating bodies in an otherwise still fluid has been a problem of intrinsic interest. In potential-flow theory, the transient response of a body with given initial displacement, say, heave or roll, would be an oscillatory motion not necessarily at a constant period. This is true even within the realm of linear water-wave theory because the hydrodynamic force contains memory effects. The issue is congruent to the fact the hydrodynamic force coefficients, such as added mass and damping, are frequency dependent. Even so, it is a common engineering practice to measure “damping” of a particular floating system by transient decay tests. The expectation is that one would then hope to capture the damping value at the “natural frequency” of the body.

A time-domain solution of free-decay motion was first obtained by Maskell & Ursell(1970) for a circular cylinder. Potential-flow solutions were obtained by Chapman (1974), Adachi and Ohmatsu (1979), Yeung (1982), the latter for a body of an arbitrary shape. Newman (1985) studied the response of a vertical cylinder of finite draft using an impulse response function. There are many recent works that involve time domain simulations (Tanizawa, 1990, Van Daalen 1993, Wu & Eatock-Taylor, 1996, Celebi & Beck, 1997). However efforts that take into account the presence of viscosity are more limited. In the absence of bilge keels or other sharp-edged geometry, roll motion decays slowly since wave damping for typical shapes would be small. Bilge keels and damping plate are often introduced to provide the necessary increase in damping to mitigate motion response.

The solution of the transient response of a floating body with keels is non-trivial since flow separation would be a significant contributor to damping. There exist empirical means of inclusion of such viscous effects (e.g., Himeno, 1981, Downie et al., 1990). Nonetheless, it would be highly desirable to remove any empiricism by including the effects of viscosity at outset of the formulation. This has been successfully pursued by Yeung and Liao (1999) by using the FSRVM (Free-Surface Random-Vortex Method) method. Experimental Validations have been reported for the case of forced oscillatory motion and for wave-induced motion. In this paper, we pursue this method further to study the decay of free roll motion of cylinders with bilge

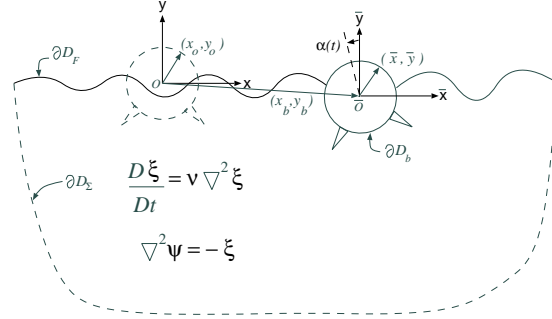


Figure 1: Definitions and the Fluid Domain Bounded by ∂D .

keels. The problem is formulated to allow full consideration of the coupling effects of the three degrees of freedom of the cylinder. The starting amplitude of roll can be large as long as the bilge keels do not emerge out of the water.

2 Method of Solution

The Free-Surface Random-Vortex Method, as introduced by Yeung and Vaidhyanathan (1994), is a Lagrangian-Eulerian description of the fluid that can take into account of fluid viscosity and free-surface motion. The theoretical formulation allows for arbitrary body shapes. A very brief exposition of the method is given below to explain how the fluid-dynamic problem is coupled with rigid-body dynamics.

Figure 1 shows a floating cylinder undergoing three degrees of freedom motion in free surface. The computational domain is designated by D , bounded by ∂D . The center of the moving body \bar{O} is given by the coordinates $(x_b(t), y_b(t))$ with respect to O , with the roll angle $\alpha(t)$ measured positive counterclockwise.

FSRVM solves the velocity field $\mathbf{u} = (u, v)$ by decomposing it into irrotational and vortical components. The rotational part is represented by vortex blobs, while the irrotational part is described by a complex-valued boundary-integral.

Thus if ξ is the vorticity normal to the Oxy plane, and ψ the stream function, the governing equations are

$$D_t \xi = \nu \nabla^2 \xi, \quad \nabla^2 \psi = -\xi, \quad (1)$$

where D_t is the material derivative and ν the kinematic viscosity coefficient.

The vorticity equation is solved by successive fractional steps of diffusion and convection. The diffusion step uses a random-walk algorithm to diffuse the blobs, but the convection step requires the consideration of the interaction of the vortex blobs and the boundary, ∂D . An $O(N)$ algorithm is used for the mutual interaction computations of the blobs. The diffusion process is assumed to be sufficiently local so that effects of the free surface are negligible.

To obtain the stream function ψ at time t , we observe

$$\nabla^2 \psi_v = -\xi, \quad \nabla^2 \psi_h = 0. \quad (2)$$

where ψ_v is known if the position and strength of each vortex blob is known and ψ_h is a solution of a boundary-value problem in D . Since ψ_h satisfies Laplace's equation, we can introduce a complex potential $\beta_h(z, t) = \phi_h + i\psi_h$, where ϕ_h is the conjugate function (velocity potential) associated with ψ_h and $z = x + iy$.

At any given time t , it follows from Cauchy's integral theorem that either ϕ_h or ψ_h can be solved on the fluid boundary when its conjugate part is specified on that part of boundary:

$$\pi i \beta_h(z) - \int_{\partial D} \frac{\beta_h(\zeta)}{\zeta - z} d\zeta = 0 \quad \text{for } z \in \partial D. \quad (3)$$

Specifically, on the body boundary, the no-leak condition can be shown to yield:

$$\psi_h = -\psi_v + \dot{x}_b \bar{y} - \dot{y}_b \bar{x} - \frac{1}{2} \dot{\alpha} R_o^2 \quad \text{on } \partial D_b. \quad (4)$$

where \dot{x}_b , \dot{y}_b , and $\dot{\alpha}$ are the rigid-body velocities of the body and $R_o^2 = \bar{x}^2 + \bar{y}^2$ for a body point with coordinates \bar{x} , \bar{y} . If z is on the free surface ∂D_F , the kinematic boundary condition for the complex velocity $w = u - iv$ is used to advance the location of the free surface, while the dynamic condition can be used to advance ϕ_h :

$$D_t z = w^*(z, t) - \nu_d(z - z_o), \quad (5)$$

$$D_t \phi_h = -D_t \phi_v + \frac{1}{2} w w^* - gy - \nu_d \phi, \quad (6)$$

Here * indicates complex conjugate. The damping function ν_d in Eqns. (5) and (6) is zero except in the damping layers $-L < x \leq x_l$ and $L > x \geq x_r$ on the left and right ends of the free surface, and z_o is the initial location of the lead free-surface node of the layers at $t = 0$.

After β_h is solved, the "no-slip" boundary condition on ∂D_b is satisfied by generating vorticity of an opposite sign to nullify the tangential surface velocity from β .

To obtain the forces and moment on the body, we need to solve for $\partial \beta_h / \partial t$, since $\partial \phi_h / \partial t$ is needed in Euler's integral to evaluate the surface pressure.

$$\frac{p}{\rho} = -\frac{\partial(\phi_h + \phi_v)}{\partial t} - \frac{1}{2} |\nabla \phi|^2 - gy, \quad (7)$$

Thus, an integral equation similar to Eqn. (3) has to be set up in parallel for $\partial \beta_h / \partial t$. The boundary conditions of $\partial \phi_h / \partial t$ on ∂D_F are given by Eqn. (6). On ∂D_b ,

$$\frac{\partial \psi_h}{\partial t} = \dot{x}_b \bar{y} - \dot{y}_b \bar{x} - \frac{1}{2} \dot{\alpha} R_o^2 - \left\{ \frac{\partial \psi_v}{\partial t} + \dot{x}_b v - \dot{y}_b u + \dot{\alpha} [(\dot{x}_b - u)\bar{x} + (\dot{y}_b - v)\bar{y}] \right\}. \quad (8)$$

Once the quantity ϕ_t is known, it follows from (7) that the hydrodynamic force $F_{1,2}$ and moment F_3 are given by

$$F_i = \int_{\partial D_b} p n_i ds, \quad i = 1, 2, 3, \quad (9)$$

where $n_1 = n_x$, $n_2 = n_y$, $n_3 = [n_x(y - y_b) - n_y(x - x_b)]$. Shear stresses on the body surface is neglected

Note that in the absence of ψ_v , the flow is entirely irrotational. Thus, a fully nonlinear inviscid solution can be recovered using FSRVM by shutting off the vorticity generation process.

The free-motion problem introduces the complexity that the body acceleration terms in Eqn. (8) are unknown and are coupled to the pressure integration of Eqn. (9) via Newton's Second Law:

$$M(\ddot{x}_b - \bar{y}_g \ddot{\alpha} - \bar{x}_g \dot{\alpha}^2) = F_1 \quad (10)$$

$$M(\ddot{y}_b + \bar{x}_g \ddot{\alpha} - \bar{y}_g \dot{\alpha}^2) = F_2 + Mg, \quad (11)$$

$$I_o \ddot{\alpha} + M(\bar{x}_g \ddot{y}_b - \bar{y}_g \ddot{x}_b) = F_3 - Mg \bar{x}_g, \quad (12)$$

where M is the body mass, and (\bar{x}_g, \bar{y}_g) the location of the center of gravity. Eqns. (10) - (12), need to be solved in conjunction with the fluid-dynamic problem described above.

In view of Eqn. (8), four new analytic functions can be constructed to represent the complex potential $\partial \beta_h / \partial t$:

$$\left(\frac{\partial \phi_h}{\partial t} + i \frac{\partial \psi_h}{\partial t} \right) = \beta_{1t} \ddot{x}_b + \beta_{2t} \ddot{y}_b + \beta_{3t} \ddot{\alpha} + \beta_{4t}. \quad (13)$$

Equation (13) indicates that β_{1t} , β_{2t} , and β_{3t} are each associated with effects due to unit body acceleration, and β_{4t} is related to known behavior of the velocity field. It is not difficult to obtain the integral equations for these four β_{it} s. None of these boundary-value problems depends on the unknown accelerations $(\ddot{x}_b, \ddot{y}_b, \ddot{\alpha})$. Thus, similar to (3), four integral equations can be set up for each of the β_{it} , $i = 1, \dots, 4$.

When the resultant ϕ_{it} terms are introduced back to the right-hand side of (10)-(12), we can separate the unknown accelerations from quantities that can be calculated. It follows then a set of coefficients A_{ij} and W_{4i} can be defined:

$$A_{ij}(t) = \rho \int_{\partial D_b} \frac{\partial \phi_j}{\partial t} n_i ds, \quad i, j = 1, 2, 3; \quad (14)$$

$$W_{4i}(t) = -\rho \int_{\partial D_b} \left(\frac{\partial \phi_4}{\partial t} + \frac{\partial \phi_v}{\partial t} + \frac{1}{2} |\nabla \phi|^2 + gy \right) n_i ds. \quad (15)$$

With the use of these coefficients, Eqns. (10-12) can be reduced to give

$$\begin{bmatrix} (M + A_{11}) & A_{12} & (A_{13} - M\bar{y}_g) \\ A_{21} & (M + A_{22}) & (A_{23} + M\bar{x}_g) \\ (A_{31} - M\bar{y}_g) & (A_{32} + M\bar{x}_g) & (I_o + A_{33}) \end{bmatrix} \begin{bmatrix} \ddot{x}_b \\ \ddot{y}_b \\ \ddot{\alpha} \end{bmatrix} = \begin{bmatrix} W_{41} + M\bar{x}_g \dot{\alpha}^2 \\ W_{42} + M\bar{y}_g \dot{\alpha}^2 - Mg \\ W_{43} - Mg\bar{x}_g \end{bmatrix}. \quad (16)$$

Equation (16) describes completely the full dynamic coupling between the fluid and body and all modes of motion. It yields $(\ddot{x}_b, \ddot{y}_b, \ddot{\alpha})$ at any given t without relying on any finite differencing scheme in time. The treatment is therefore fully implicit and stable.

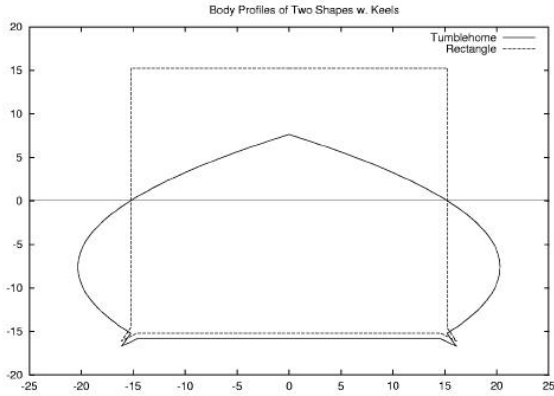


Figure 2: Body Profiles for a Rectangular Section and a Tumblehome Section

3 Results and Discussion

Figure 2 shows two body sections to which the method of solution in Section 2 is applied. One is a rectangular body, the other a tumblehome-shaped body with a flat bottom. Both have beams of 30.5cm. These are overlaid to indicate their relative dimensions. The bilge keel depth to half beam ratio, K_D , is 0.079. The reference period T for roll is 1.958 seconds. Figure 3 shows the slow roll decay of both cylinders from an initial angle of 10° in an inviscid fluid. It seems puzzling that the tumblehome-body motion decays faster than the rectangular shape, since it is more rounded and its keels are at about the same location. The explanation for this is related to the frequency dependency of the damping. Figure 4 shows the linear, wave damping λ_{33} of the two sections versus $\tilde{\omega} \equiv \omega \sqrt{B/2g}$. It is clear that based on the “crude” oscillation frequency of the two bodies, rectangular section, $\tilde{\omega} = 0.64$, tumblehome section, $\tilde{\omega} = 0.49$, the latter has a much higher amount of damping. Note that the period of oscillation is not constant, increasing somewhat slowly in time.

In an inviscid fluid, a circular cylinder would oscillate indefinitely in roll in the absence of any bilge keels. Figure 5 shows the decay of motion due to the generation of surface waves by a pair of 10%-keels ($K_D = 0.1$), which are positioned at the $\pm 45^\circ$ position of the circular cylinder. The roll angle is $+40^\circ$ at $t = 0$ with no heave and sway displacement. The cylinder, with a beam of 30.5 cm, was in static equilibrium with $\bar{y}_G/B = -0.197$. In an inviscid fluid, the decay is slow. The nonlinear coupling of the motion modes gives rise to heave motion occurring roughly at the “natural heave frequency”. Sway and roll coupling leads to an oscillatory sway response that approach a constant. The large-time static drift is about 10% of the radius.

Figure 6 shows the corresponding response for a viscous fluid ($\nu = 1.14 \times 10^{-2} \text{ cm}^2/\text{sec}$). The bilge keels generate so much damping that the roll maxima are almost halved in successive periods initially. A larger sway drift is observed. The roll and sway responses with and without viscosity during the initial few periods are compared more vividly in Figure 7.

A rectangular cylinder with bilge radius being 2.1% of its beam was ballasted with a $\bar{y}_G = -4.53 \text{ cm}$ ($B = 23.54 \text{ cm}$). The sharp corners produce significant viscous

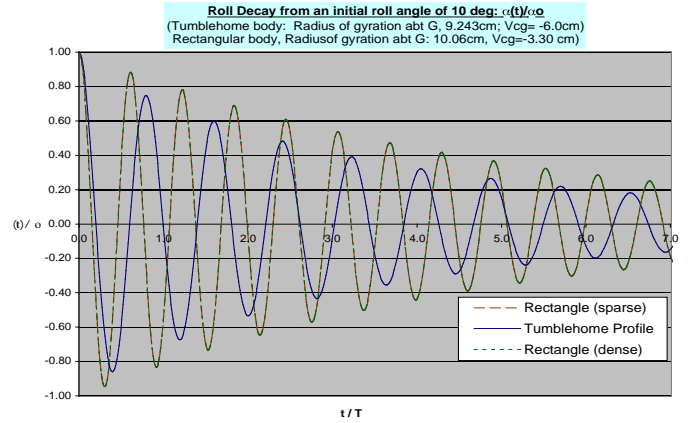


Figure 3: Time History of Roll for Rectangular and Tumblehome Bodies

damping besides wave damping. Figure 8 shows the configuration of the cylinder in equilibrium in laboratory condition. It is allowed to roll about the waterline. The comparison between the experimental measurements and the predictions of FSRVM is shown in Figure 9. The agreement with the viscous-fluid model is excellent for the first four periods. For large time, and small angle of roll, the assumption of a frictionless rotary bearing is not quite applicable.

4 Conclusions

A theoretical study of the roll decay of cylinders is presented. The study examines the viscous effects on the decay, which are substantial for bodies with bilge keels. In the 3DOF coupled system, the body is seen to drift slightly in a direction of the higher initial position of the two keels for the cases investigated. The decay rate is well substantiated by an experiment for a rectangular cylinder conducted at University of California, lending much credence to the method of solution.

5 References

- Adachi H. and Ohmatsu, S. (1979). *Proc. 13th Symp. on Naval Hydrodyn.*, Tokyo, pp. 281-299.
- Chapman, R. B. (1979). *Journal of Ship Research*, **23**, pp. 20-31.
- Celebi, M. S. and Beck, R. F. (1997). *Journal of Ship Research*, **41**, pp. 17-25.
- Downie, M., Graham, J. and Zheng, X. (1990). *Proc. 18th Symp. on Naval Hydrodyn.*, Ann Arbor, Michigan, pp. 149-155.
- Himeno, Y. (1981). Dept. Naval Arch. & Mar. Engrg., University of Michigan, Rep. no 239.
- Maskell, S. J. and Ursell F. (1970). *Journal of Fluid Mech.*, **44** pp. 303-313.
- Newman J. N. (1985). *Journal of Fluid Mech.*, **157**, pp.17-33.
- Tanizawa, K. (1990). *Journal of Soc. Naval Arch. Japan*, **168**, pp. 221-226.
- Van Daalen, E. F. G. (1993). Ph.D. dissertation, University of Twente, The Netherlands.
- Wu, G. X. and Eatock-Taylor, R. (1996). *11th Int'l Workshop on Water Waves and Floating Bodies*, Hamburg, Germany.
- Yeung, R. W. (1982). *Journal of Engrg. Math*, **16**, pp. 97-119.
- Yeung, R. W. and Liao S.-W. (1999). *Proc. 9th Int'l Offshore and Polar Engrg. Conf.*, Brest, France.
- Yeung, R. W. and Vaidhyanathan, M. (1994). *Proc. Int'l Conf. on Hydrodyn.*, Wuxi, China.

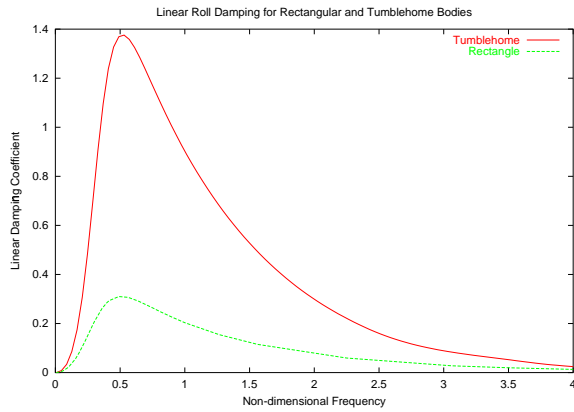


Figure 4: Linear Roll Damping for Rectangular and Tumblehome Bodies as Functions of $\tilde{\omega}^2$.

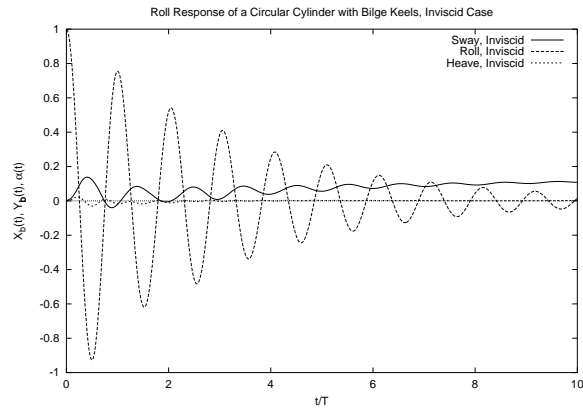


Figure 5: Roll, Sway and Heave response of a Circular Cylinder, $K_D = 0.1, \alpha_o = 40^\circ$ - Nonlinear Inviscid Solution.

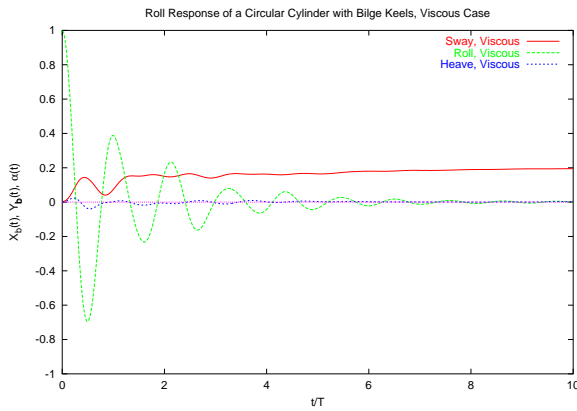


Figure 6: Roll, Sway and Heave response of a Circular Cylinder, $K_D = 0.1, \alpha_o = 40^\circ$, with Viscosity.

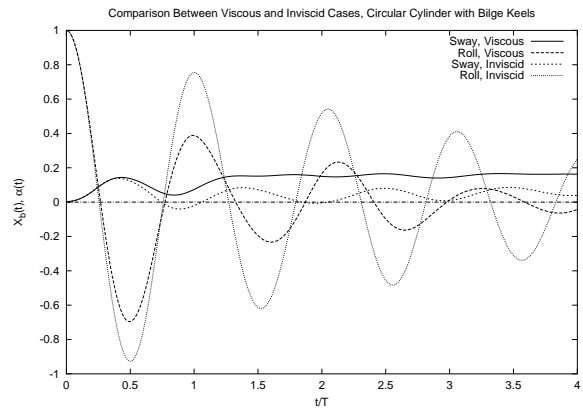


Figure 7: Comparison of Time Histories, Inviscid vs Viscous Fluid.

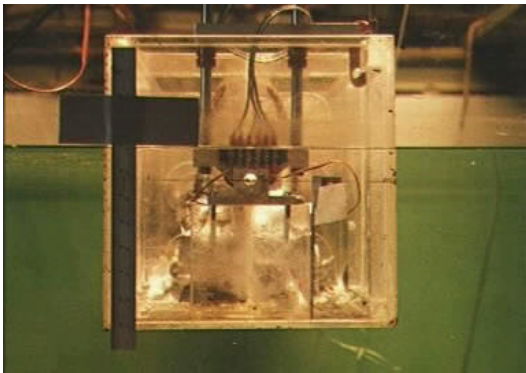


Figure 8: Laboratory Experiment of a Cylinder for Roll Decay Test.

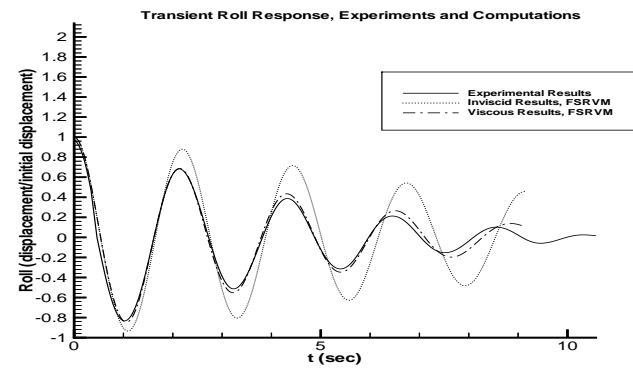


Figure 9: Transient Roll Decay of a Rectangular Cylinder without Bilge Keels, Experiments and Theory.